Increase of charge-carrier redistribution efficiency in a laterally organized superlattice of coupled quantum dots

C. Cornet,[1,*] M. Hayne,[2,†] P. Caroff,[1] C. Levallois,[1] L. Joulaud,[1] E. Homeyer,[1] C. Paranthoen,[1] J. Even,[1] C. Labbé,[1] H. Folliot,[1] V. V. Moshchalkov,[2] and S. Loualiche[1]

[1]*LENS-UMR FOTON 6082 au CNRS, INSA de Rennes, 20 Avenue des Buttes de Coesmes, CS 14315, 35043 Rennes Cedex, France*

[2]*INPAC-Institute for Nanoscale Physics and Chemistry, Pulsed Field Group, Katholieke Universiteit Leuven, Celestijnenlaan 200D, B-3001 Leuven, Belgium*

(Received 23 November 2005; revised manuscript received 5 September 2006; published 18 December 2006)

We report the observation of enhanced charge-carrier redistribution in laterally organized and coupled InAs/InP quantum dots (QDs). We show that a periodic organization appears in the QD plane for a high in-plane QD density (QDD). This organization enhances the lateral coupling between the dots, which is evidenced by photoluminescence and magnetophotoluminescence experiments. Electronic inter-QD lateral coupling results in an improved charge-carrier distribution at low temperature, as shown by electroluminescence on high QDD QD lasers. We conclude that the inter-QD tunneling occurs via the tunneling of excited states through the wetting layer, and discuss the prospects of using coupled QDs for improving the quantum efficiency and dynamical properties of QD lasers.

DOI: 10.1103/PhysRevB.74.245315 PACS number(s): 73.21.La, 68.65.Hb, 73.63.−b, 78.20.Ls

I. INTRODUCTION

Recently, there have been considerable research developments in the field of nanostructured semiconductor materials. In particular, quantum dots (QDs) may improve the properties of high-performance optoelectronic devices as compared to that achieved with semiconductor quantum wells.[1–4] On one hand, many studies have been performed on single QDs as single-photon emitters,[5,6] or independent QDs for optoelectronic devices.[7] Recently, double quantum dots (two laterally coupled QDs) have been developed for applications in quantum computation.[8] On the other hand, vertically coupled QDs were used in order to improve QD laser characteristics,[3] as well as a basis for quantum processors.[9] In all these devices, the problem of carrier injection is of prime importance. The main challenge is to distribute the charges to the maximum number of QDs, with the minimum of energy, implying that we should reach the highest possible charge-carrier redistribution efficiency in these systems. To date, carrier redistribution between QDs has been almost exclusively discussed in terms of thermally mediated processes in which carriers localized in the QDs are excited to the two-dimensional wetting-layer (WL) continuum.[10,11] In the widely studied InAs/GaAs system, this is a very reasonable assumption since the thickness of the WL is typically substantially smaller than the height of the dots, therefore the confinement energy is much higher, and the WL states are separated by ~200 meV from the QD ground state. Thus lateral electronic coupling between dots via WL states (tunneling) is usually neglected in the simulations.[10,11] However, in the InAs/InP system the typical height for QDs emitting at a wavelength of 1.55 μm is about 3 nm, while the typical height for the wetting layer is about 1 nm. Thus the wetting-layer continuum states are energetically closer to the QD ground state in such a system (~150 meV). Hence, the effect of lateral coupling should be considered. In order to model an infinite superlattice of QDs, an original method based on the resolution of the Schrödinger equation in the reciprocal space was developed independently by Gunawan *et al.*[12] and our group.[13] Results presented in Ref. 13, part IV, modeled for a real sample, show that lateral coupling effects may occur for such a high QDD. This would have two related consequences: the lateral delocalization of zero-dimensional (0D) QD states, and eventually, miniband effects on previously quantized QD energy levels, giving rise to a splitting of both degenerate p and d states as the QDD increases. These calculations also described three different regimes of coupling. (1) The uncoupled regime occurs when the density of QDs is low. Here, QDs are electronically independent, with neither miniband effects nor delocalization of the wave function observable. In this regime, the only way for an electron in the ground state of one QD to reach another QD, is to get enough (thermal) energy to get over the barrier energy levels. This is the typical regime for QD samples, particularly those in the InAs/GaAs system. (2) For a higher QDD, wetting-layer-assisted inter-QD coupling can occur. This is an intermediate coupling regime. Slight delocalization of the wave function appears for ground state as a precursor to miniband effects, which are stronger and stronger for higher-energy states. This means that while the ground state keeps its zero-dimensional characteristics, excited states become hybrid zero-dimensional/two-dimensional states with a large spatially localized component in the QDs, but extend across the sample through the WL. Thus, in order to travel to another QD, an electron in the ground state of one QD needs only enough energy to reach excited states of the QD, and can then tunnel through the WL to another QD. (3) The direct inter-QD coupling regime occurs for very high QDD. In this strong-coupling regime all QD energy levels have large miniband effects and delocalized wave functions. In this case, every electron in the ground state of a QD can thus tunnel directly to another QD ground state.

In the present work, we experimentally investigate an organized superlattice of coupled dots in order to show efficient charge-carrier redistribution between QDs. It is demonstrated that for high quantum dot densities (QDD), an in-

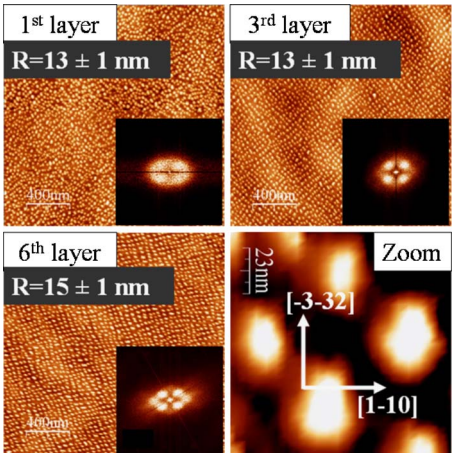

FIG. 1. (Color online) AFM pictures (2×2 μm) of three samples with 1, 3, and 6 stacked QDs layers, respectively. A zoom of the AFM picture of the six-stacked-QD-layers sample is also shown with corresponding crystallographic directions. The average QD radii are also given. The insets represent the corresponding two-dimensional Fourier-transformed pictures, showing the influence of stacking on lateral organization at high QD densities.

plane periodic organization appears. Based on previous calculations,[13] we describe how this superlattice configuration leads to inter-QD lateral coupling, and how this lateral coupling can be probed by photoluminescence experiments. The consequences of coupling on the Bohr exciton radius and electronic structure of the dots are observed with magnetophotoluminescence and high-power polarized photoluminescence experiments. Improved charge-carrier redistribution at low temperature in a high QDD sample is revealed by electroluminescence experiments. We discuss how the lateral coupling improves charge-carrier redistribution, and conclude that the coupling is due to inter-QD tunneling of excited states via the wetting layer.

Before presenting our work, a point of information seems to be necessary on the large variety of samples studied here. Magnetophotoluminescence is first performed at 4 K on the single dot layer in order to evidence the lateral coupling. However, in order to avoid any water absorption (around 0.9 eV), the samples used here are designed to emit around 0.8 eV at 4 K. High-power photoluminescence is then performed at room temperature (RT) because no cryostat is available on this experiment. For the same reasons, the samples used here are designed to emit around 0.8 eV at RT. Then, electroluminescence experiments are performed on QD laser guides. In these laser guides, 3 stacked QD layers are used in order to reach enough gain for the laser emission. QDs are then designed to emit at 0.8 eV at RT. In order to compare all the results presented here, we study in the first part the effect of the stacking process on QD density, size, shape, and distribution.

II. GROWTH OF QUANTUM DOTS SUPERLATTICES

Recent growth developments in our group have allowed us to vary the QDD, and to reach very high QDD.[13,14] This

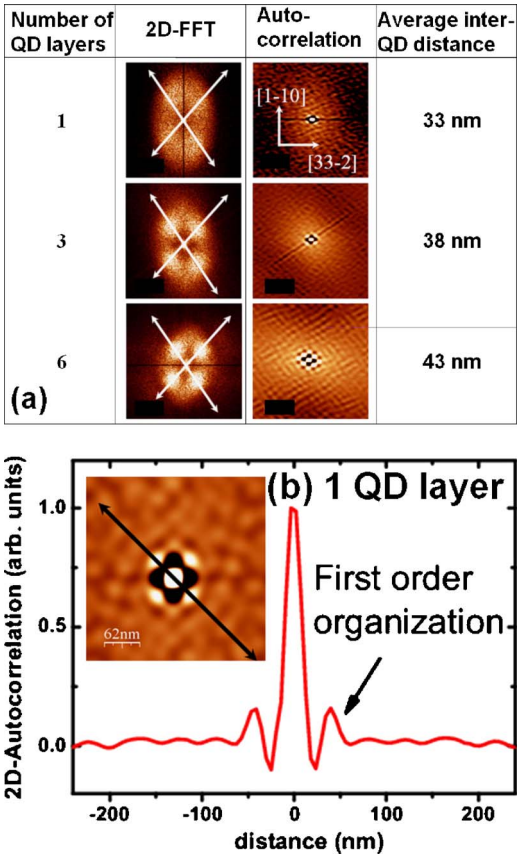

FIG. 2. (Color online) (a) Table representing the 2D Fourier-transformed pictures, autocorrelation pictures, and inter-QD average distance as a function of the number of stacked QD layers. (b) A cross-sectional projection of the 2D autocorrelation shows the short-range ordering of the QDs even with one QD layer.

research is devoted to the study of the InAs/Q1.18 QD system on a (311)*B* InP substrate, where Q1.18 is the quaternary alloy $In_{0.8}Ga_{0.2}As_{0.435}P_{0.565}$, emitting at a wavelength of 1.18 μm at room temperature. By decreasing the As flux, and with the same amount of InAs deposited, the QDD can increase as high as 1.6×10^{11} cm^{-2}. Figure 1 is an atomic-force microscopy (AFM) picture of three samples, grown with low As flux, with 1, 3, and 6 stacked QD layers, respectively, separated with a 40 nm Q1.18 spacer. An ultrasharp AFM tip with a typical tip radius <10 nm is used in order to avoid tip effects in the image. As shown in Fig. 1, the more stacked QD layers the sample has, the more the QD layers become organized. The presence of QD self-organization is clearly shown by the observation of intensity spots on the two-dimensional fast-Fourier-transformation (2D FFT) picture presented in the insets of Fig. 1. This QD organization is enhanced by increasing the number of stacked QD layers, but AFM measurements show that it is already present from the first QD layer, and becomes strong on the third QD layer. Figure 2(a) presents the 2D FFT, autocorrelation, and inter-QD average distance a for uncapped versions of all the samples in this investigation. The autocorrelation is of prime importance here, as it allows us to quantify the ordering of the sample. As can be seen from autocorrelation pictures [Fig. 2(b)], the single-layer sample has a short-range organi-

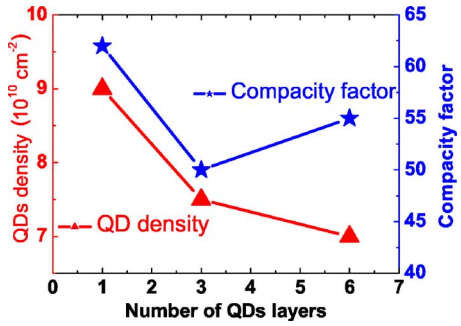

FIG. 3. (Color online) Evolution of the compacity factor and QD density as a function of the number of stacked QDs layers.

zation (at least first order), while the sample with six stacked QD layers has a long-range organization (at least sixth order). This phenomenon has already been shown and explained by Xu *et al.*,[15] who demonstrated that, even for a single layer, an organization can appear when a high QD density is reached, and especially for samples grown on (311)B substrates. For such substrates the islands tend to order themselves along the direction of the smallest Young's modulus, i.e., along the smallest deformation direction. It can also be understood in the following way: For such a high QDD sample, a disordered nucleation would lead to a large energetic waste. Thus, a periodic organization appears in the QD plane, in order to minimize the surface energy.[16] In multiply stacked layers this organization is enhanced by the strain field induced by the first QD layer. This has been demonstrated by Tersoff *et al.* who modeled the stress field in stacked QDs.[17] The zoom presented in Fig. 1 shows that the QDs are elongated along the [3 3 −2] direction, while the lattice direction of 2D self-organization is aligned along a direction of minimum deformation (about 45° from the [3 3 −2] direction). As these QDs have an anisotropic shape, polarization of the luminescence is expected.

Figure 3 shows the evolution of QD density, and of the compacity factor,[13] $C=\pi R^2/a^2$ (i.e., the surface coverage) as a function of the number of QD layers measured from AFM. The corresponding radii are given in AFM pictures of Fig. 1. All the values presented here have been extracted from the AFM pictures using "SPM-image magic" software. As we use an ultrasharp AFM tip, and as the vertical aspect ratio of our QD is very low (uncapped QDs have more or less a 5 nm height), the AFM image is assumed to be uninfluenced by tip effects, and an accurate mean dot size is determined. As shown in Fig. 3, the QD density decreases with an increasing number of QD layers, although it remains high (between 7×10^{10} and 9×10^{10} cm^{-2}). The compacity factor, which is determined as the ratio of area occupied by the dots on the AFM images of Fig. 1 to the total image area, decreases as the number of QD layers decreases from 1 to 3 (the dots have the same radius, but the density decreases). It then increases as the number of QD layers increases from 3 to 6 (the density is nearly constant while the mean radius increases). In Fig. 4 we compare the lateral organization in samples with six stacked layers and (a) low or (b) high QDD. It can be seen that the high QDD sample shows a large degree of lateral ordering, whereas it is absent in the low QDD sample. This clearly demonstrates that although the lateral ordering is amplified by stacking the QD layers, its origin lies in the high QDD.

III. LATERAL COUPLING BETWEEN QUANTUM DOTS

A. Magnetophotoluminescence

One way to probe the lateral extent of the wave function in the QD is to perform photoluminescence (PL) with a high magnetic field applied along the growth direction. Magneto-PL experiments were carried out at 4.2 K in a He bath cryostat placed in the bore of a pulsed magnet with a maximum field of 50 T.[18] The field was applied parallel to the growth direction (z). A single 550 μm core optical fiber was used to collect the PL signal, which was excited by the light from a cw frequency-doubled Nd:yttrium-aluminum-garnet (YAG) laser at 532 nm via a second fiber. A cooled InGaAs linear diode array coupled to an optical spectrum analyzer is used to detect the PL. Samples used in this experiment are low and high QDD samples with one QD plane, designed to emit around 0.8 eV at 4.2 K. QDD for both samples are assumed to be similar to those measured by AFM measurements in part II. The impact of a magnetic field on QD samples has been already studied.[18,19] Following an excitonic model, at zero and low magnetic fields, the electron and hole within the dot are strongly spatially confined by the physical boundaries of the dot. In these conditions, the magnetic field can be treated as a perturbation in the Hamiltonian, leading to a square dependence of the energy shift on

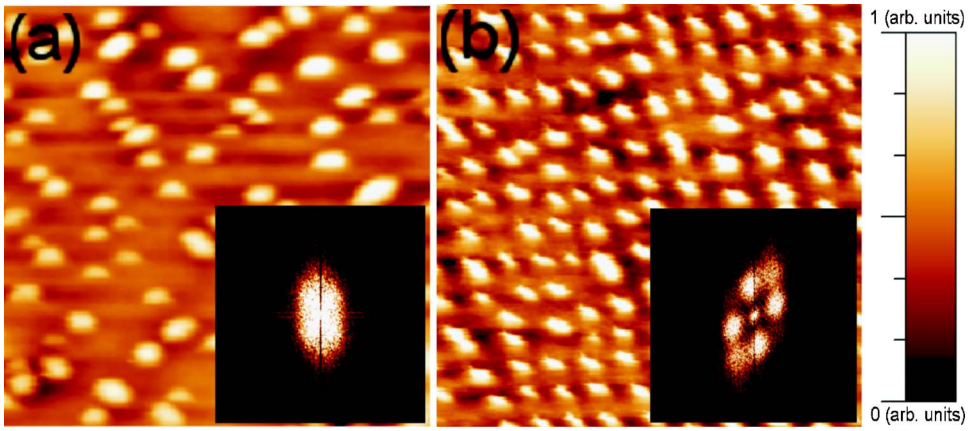

FIG. 4. (Color online) AFM pictures (0.5×0.5 μm) of samples with six stacked layers and (a) a low QD density of 4×10^{10} cm^{-2} and (b) a high QD density of 8×10^{10} cm^{-2}. Bright areas represent the maximum height of the dots (i.e., about 6 nm). The insets show the corresponding two-dimensional Fourier-transformed pictures, demonstrating the presence of lateral organization only at high QD densities.

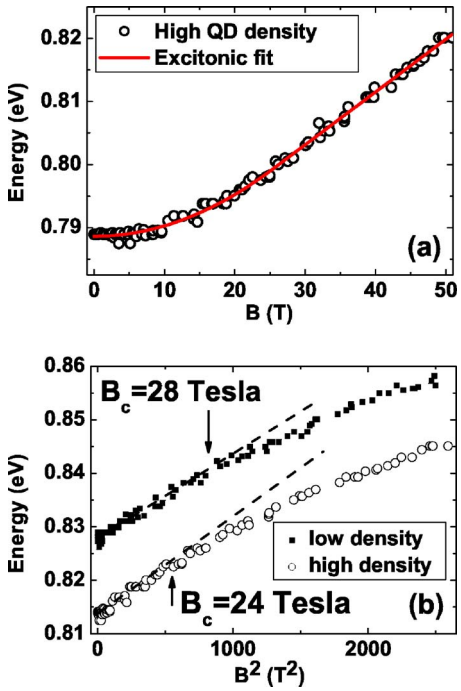

FIG. 5. (Color online) (a) Evolution of the luminescence peak as a function of the magnetic field applied in the growth direction for the high QD density sample with associated excitonic fit. (b) Evolution of the luminescence peak as a function of the magnetic field squared for low and high QD density samples (shifted for clarity). The crossover between the linear and nonlinear regime is directly linked to the spatial extent of the wave function, and is indicated by an arrow in each case. The lower crossover field for the laterally smaller QDs in the high QD density sample is evidence of electronic coupling.

the magnetic field: $\Delta E = e^2\langle\rho^2\rangle B^2/8\mu_r$,[18] for $B < B_c = 2\hbar/e\langle\rho^2\rangle$, where $\sqrt{\langle\rho^2\rangle}$ is the in-plane effective exciton radius (Bohr radius), μ_r is the in-plane exciton effective mass, B is the magnetic field, and B_c is the crossover magnetic field, which depends only on $\sqrt{\langle\rho^2\rangle}$. This diamagnetic dependence at a low magnetic field can be seen in Fig. 5(a). At a sufficiently high field ($B > B_c$), when the attempted Larmor radius is smaller than the spatial size of the dot, the charges become confined by the field in the plane perpendicular to the direction on which it is applied, and the energy levels shift linearly with B: $\Delta E = \hbar eB/2\mu_r$.[18] The linear dependence at a high magnetic field can also be seen in Fig. 5(a). Using this model, knowledge of B_c directly gives us the value of $\sqrt{\langle\rho^2\rangle}$. Figure 5(b) shows the evolution of the photoluminescence peak energy as a function of B^2. At low B, the diamagnetic shift of the transition is shown by the linear dependence of the PL energy on B^2 in the figure. However, at high B, the dependence on B^2 is no longer linear. The values of B_c deduced by fits of the measurements with the expressions of the excitonic model [Fig. 5(a)] are reported on Fig. 5(b). As we only look at the evolution of the ground-state transition, and do not consider the intensity variations, effects of different charge-carrier-state filling on the two different QDD samples are not considered here. Indeed, recent calculations have shown that, at least in the GaAs/Al_xGa_{1-x}As system, the influence of different dot charge states on the shift of ground or excited state PL with magnetic field is negligible.[20] The corresponding exciton Bohr diameters are thus equal to 13 nm for the low QDD sample, and 15 nm for the high QDD sample. Assuming the low QDD sample as a reference, we can define the standard confinement coefficient in our QD as $\Gamma_0 = D_{X0}/D_{D0}$, where D_{X0} and D_{D0} are the exciton Bohr diameter and the measured AFM diameter, respectively, of QDs on the low QDD sample. From the measurements presented in Fig. 2, we can calculate the coupled confinement coefficient defined as $\Gamma_C = D_{XC}/D_{DC} = 1.5\Gamma_0$, where D_{XC} and D_{DC} are the exciton Bohr diameter and the measured AFM diameter, respectively, of QDs on the high QDD sample. This result shows that for a high QDD, the wave function expands even though the structural size of the dots is smaller. In a strong confinement regime,[1,21] this could be explained by wave-function spillout in the barrier, due to the proximity between the QD ground-state energy and the barrier energy. This has been shown in Ref. 21 in the InAs/InP system, where it was found that when the confinement is weak, i.e., when the typical dimension of the nanostructure is larger than eight monolayers (about 2.5 nm), increasing the size of the nanostructure results in an expansion of the wave function. However, when the confinement is strong, i.e., when the typical dimension of the nanostructure is smaller than eight monolayers, then the smaller the nanostructure, the larger the wave function. Here, with typical diameters of about 30 nm for our QDs, the lateral confinement is very weak, and we are very far from the strong confinement regime. Thus, we interpret the delocalization of the wave function as a direct consequence of the lateral coupling, as predicted by the calculations in Ref. 13. Unfortunately, the excited states of our QDs cannot be probed with our high-field experimental setup: at the available pumping energy the sample burns before we can reach high enough QD occupation densities. However, standard PL measurements performed with another pump laser provide evidence of highly delocalized excited states.

B. High-excitation power photoluminescence

Photoluminescence experiments with high-power optical injection and polarization-sensitive detection have been performed on both low and high QDD samples. The samples used have one QD plane, and are designed to emit around 0.8 eV at RT. High-power PL experiments were carried out at RT. The luminescence was excited with a YAG laser at 1.06 μm, which was focused on the sample with a microscope objective, leading to a maximum excitation power of 170 kW cm^{-2}. An InGaAs detector was used, coupled to an optical spectrum analyzer. The aim of this experiment is to identify the PL ground- and excited-state energies in our system with good accuracy, rather than to study the state filling as a function of laser power in low and high QDD samples. Moreover, as the anisotropic shape of the QDs (see part II) leads to a polarization dependence of the zero-field PL, polarization sensitivity is used. Indeed, in such an anisotropic QD, the wave function should become aligned with its maximum extent along the [3 3 −2] direction, and a smaller spa-

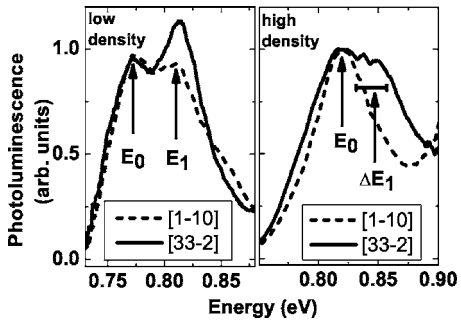

FIG. 6. Polarized photoluminescence under high-excitation power (170 kW cm^{-2}). The low QD density sample shows an energy difference between ground- and excited-state transitions of 41 meV (a), while the high QD density sample shows a miniband effect in the excited state and an energy difference between ground- and excited-state transitions of 23 meV (b).

tial extent along $[1-1\ 0]$. Considering that the strongly localized ground state has the $1S$ symmetry, it should be relatively insensitive to the QD anisotropy. On the other hand, the excited $1P$-like states are expected to be very sensitive to the anisotropic QD geometry: the excited-state luminescence polarized along the $[3\ 3-2]$ is expected to have a greater oscillator strength than the luminescence polarized along the $[1-1\ 0]$. Figure 6 shows photoluminescence spectra for low [Fig. 6(a)] and high [Fig. 6(b)] QDD samples with an excitation density of 170 kW cm^{-2}. In each case, both $[3\ 3-2]$ and $[1-1\ 0]$ polarizations are plotted, and as expected, we find no polarization of the ground state, whereas the excited state is partially polarized in the $[3\ 3-2]$ direction. For the low QDD sample there is little difference in the peak energies for the two polarizations, and the difference between excited- and ground-states transitions $\Delta E=E_1-E_0=41$ meV. This measurement also allows the determination of the WL luminescence at 0.94 eV and the matrix material at 1.18 μm (1.05 eV) at RT, which are not shown here for clarity. The excited-state transition has a full width at half maximum (FWHM) of 27 meV. For the high QDD sample, the excited-state transition appears changed in its shape. Instead of being well defined, the excited-state transition is wider and closer to the ground-state transition. By taking a mean value for the excited-state transition, the difference between ground- and excited-state transitions is found to be $\Delta E_c=23$ meV. This observation can be understood as a consequence of lateral coupling. Indeed, QDs with a large radius usually have their excited states closer to the ground state than QDs with a small radius. We measure exactly the opposite, which we attribute to a direct consequence of the lateral coupling between dots,[13] as we did for the exciton Bohr radius discussed in Sec. III A above. Furthermore, the FWHM of this transition is about 38 meV. This enlargement of the transition is attributed to a miniband effect, again as a consequence of inter-QD lateral coupling. The model used in Ref. 13 also predicts a splitting of energy levels associated with the initially degenerate p states and d states. In these measurements, the splitting of excited states is not that clear, even if two peaks appear in Fig. 6(b). If we take a look at the ground state, then no miniband effect can be clearly distinguished. The weak delocalization of the wave function and the lack of significant miniband effect on the ground state is, though, still generally consistent with the calculations performed on this system, and leads us to consider our system to be in the intermediate coupling regime (WL-assisted inter-QD coupling). The main point demonstrated here is that the low QDD sample and the high QDD sample have a different optical signature, with evidence of miniband effects, and a shift of the excited-state energy levels in the high QDD sample. These data, combined with the magneto-PL results strongly suggest lateral coupling of the QDs via the excited states.

IV. IMPACT ON CHARGE-CARRIER REDISTRIBUTION

A. Laser spectral width

In Sec. III we presented several pieces of evidence for lateral coupling between QDs. Such a phenomenon is expected to have an influence on inter-QD charge-carrier redistribution, which we now discuss. Inter-QD charge-carrier redistribution is typically attributed to thermal excitation of electrons and holes in QDs over the barriers (including the wetting layer),[22] and may be modeled with rate equations.[10] However, while these models allow the quantification of the impact of redistribution processes on laser performance, they are based on a number of assumptions, and require the choice of certain parameters. In our case, our results show that thermal diffusion is not the only way to redistribute electrons and holes, but that electronic coupling (tunneling) has also to be considered.[23] This would introduce a further level of complexity into the construction of a rate-equation-based model. For this reason we will limit ourselves to a qualitative description of the way the carriers redistribute, which we have studied using electroluminescence experiments that we now go on to discuss.

Samples with triply stacked layers of QDs have been designed with high precision to have exactly the same QD height, i.e., the same wavelength emission. On the basis of these optimized QD layers for both low and high QDD, broad-area lasers with 100 μm stripe width were then processed. After thinning down the substrate to less than 100 μm, the structures were cleaved with lengths of 3 mm. The facets were left uncoated. Broad-area lasers were tested at different temperatures from 110 to 300 K under pulsed operation (0.5 μs pulse width, 2 kHz repetition rate).[24] Thus, electroluminescence has been performed on both high and low QDD QD-laser guides at 110 K,[24] which is the lowest temperature that can be reached on our electroluminescence setup. At this temperature, $k_bT=9$ meV, so is much smaller than typical energy differences between our QDs states. 110 K electroluminescence spectra for the high QDD QD laser (C_{T0}), and low QDD QD laser (U_{T0}) under electrical-injection currents corresponding to 1.5 times the threshold current are presented in Fig. 7. A very large difference in spectral width between the two samples can be observed. Since the lasers are multimode, the electroluminescence consists of a large number of sharp lines, giving a "noisy" spectrum. For this reason, rather than using the FWHM to characterize the spectral width, we have chosen a definition of

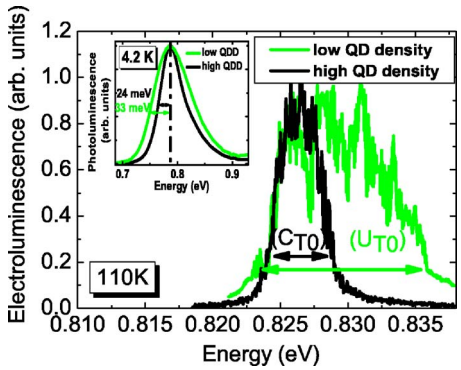

FIG. 7. (Color online) Laser emission measured using electroluminescence at 110 K for high and low QD density QD lasers. The observed spectral width reveals a large difference between the two lasers. The inset shows photoluminescence emission for high and low QD density samples at 4.2 K. The observed spectral width is similar for the two samples, and cannot account for the difference in spectral width of the electroluminescence.

spectral width corresponding to the full width at one tenth of the maximum intensity. With this definition the spectral widths are measured to be 5.5 and 13 meV for the high and low QDD samples, respectively, with an error bar of about 1 meV. Electronic coupling aside, and assuming that at this temperature we avoid an important contribution from thermal effects (i.e., the thermal redistribution), the only difference between the two samples should be the consequence of any inhomogeneous broadening. However, the FWHM measured from PL measurements on these samples are 48 meV for the high QDD sample and 66 meV for the low QDD sample [Fig. 7 (inset)]. This gives a ratio of inhomogeneous broadening for the two samples of only 1.4, compared with 2.4 for the electroluminescence spectra of Fig. 7. Figure 8 shows the evolution of the laser spectral width with temperature for an injection current of 1.5 times the threshold current at each temperature. As we can see, while the high QDD sample has nearly constant spectral width of about 5 meV, the spectral width of the low QDD sample strongly decreases as the temperature is raised to 180 K, and is nearly constant between 180 and 300 K.

Figure 9 is a schematic representation of the two competing redistribution mechanisms for (a) uncoupled dots and (b) coupled dots. The first one is the direct thermal redistribution R_T: a carrier in the ground state of one QD can be thermally excited to the barrier (Q1.18), and captured by another QD. This process has been studied experimentally by Lobo *et al.* for various InGaAs/GaAs QDD.[25] The R_T process thus needs enough energy to bring a carrier from the ground state to the barrier. The second mechanism is the tunneling redistribution via WL-assisted inter-QD coupling R_C. In this case, a carrier in the ground state of one QD can reach the higher energy states (hybrid 0D/2D states), helped by the temperature, and can then tunnel to another QD. The R_C process needs less energy than the R_T process, because of the proximity of excited states to the ground state as compared to the barrier height. In these diagrams, the probability densities associated with each energy state are represented with a gray scale. Black stands for a probability 1 and white stands for a probability 0. While for uncoupled dots a large Q1.18 barrier without low-energy states is seen by the electron, the coupled QD energy diagram reveals extended minibands on excited states. Theses states are considered as hybrid states, extended throughout the WL, but with a major component localized in the QDs.[13] With these two mechanisms in mind, Fig. 8 can have a complete interpretation. Between 180 and 300 K both R_T and R_C are efficient: No difference can be found in spectral widths between the two samples, as R_T is active in both samples. At lower temperatures (110 to 180 K) R_T becomes weaker. So, for the low QDD sample, carrier redistribution becomes inefficient as R_C is absent. As a consequence the

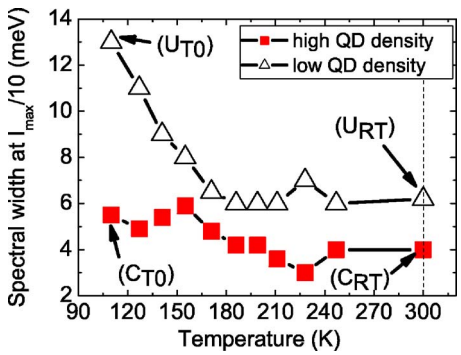

FIG. 8. (Color online) Laser spectral width at several temperatures for the high and low QD density samples. Coupling effects can be seen in the reduced spectral width for the high QD density sample at low temperature.

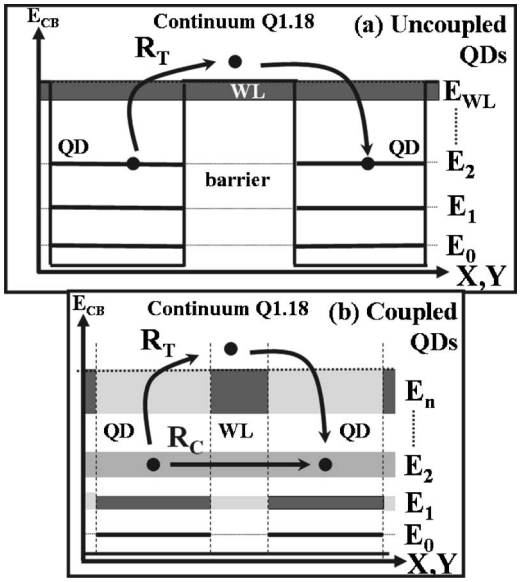

FIG. 9. Schematic representation of the conduction-band energy diagram for (a) uncoupled QDs and (b) coupled QDs along the lateral direction x,y. The inequivalent sizes of (a) and (b) in the (x,y) plane reflect the QD size and density in the two samples. The electron probability density associated with the energy levels is represented with a gray scale (white=0 and black=1). Two redistribution processes are depicted: thermal redistribution R_T and the WL-assisted tunneling redistribution R_C. In the uncoupled configuration (a) R_T is present, while for the coupled case (b) both R_T and R_C are present.

spectral width starts to increase. For the high QDD sample, R_T becomes weaker, but carriers can still redistribute efficiently via R_C. Finally, in the low-temperature limit (0–110 K), we may expect to see the spectral width of the high QDD sample increase as R_C also becomes thermally locked.

B. Discussion

We have reported a range of measurements on high QDD InAs/InP samples, which lend strong support to the presence of WL-assisted coupling, as described theoretically in Ref. 13. However, there are two aspects of the real experiment discussed here, which need to be carefully examined in the context of the calculations in Ref. 13, which are for ideal samples. These are the effects of inhomogeneous broadening in the samples, and the extent of wave-function overlap between states in real samples.

The inhomogeneous broadening in our QD samples results in different energy levels from one dot to another. The impact of such an inhomogeneous broadening on lasing and thermal redistribution properties has already been studied.[10,11] Grundmann has demonstrated that if the inhomogeneous broadening is much larger than the homogeneous broadening, then the QDs lase independently.[11] Conversely, if the homogeneous broadening becomes much more important than the inhomogeneous broadening, QDs lase in the same mode. In our case, the inhomogeneous broadening is much larger than the homogeneous broadening (see PL spectra in Fig. 8). However, we have shown in Sec. III B that miniband effects appear in the excited-states levels, which is equivalent to an increase of the homogeneous broadening of the excited states. This has the desired effect on the carrier redistribution, but since the ground state remains δ-function like (i.e., the inhomogeneous broadening is still predominant), no consequences are expected for the ground-state lasing properties.

The inhomogeneous broadening will also have an impact on the coupling properties. Coupling (tunneling) is observed when the identical energy levels of two quantum-mechanical systems which are separated by a barrier come sufficiently close. In the case of self-assembled QDs, coupling is typically considered in the context of the ground states of vertically stacked dots, separated by a thin layer of matrix (barrier) material. A number of groups have reported coupling of, for example, vertically stacked InAs/GaAs,[26] InAs/InP,[27] InP/GaInP,[28] and InGaAs/InGaAsP (Ref. 29) dots. Coupling occurs even though it is clear that the dots are not identical, although they may be very similar. This can be more easily understood bearing in mind that some small penetration of the dot wave function into the barrier can be expected, and that when two (nonidentical) dots are sufficiently close, the system can be considered as a single large QD. The point is that the dots do not have to be identical for coupling to occur, and that inhomogeneous broadening does not necessarily completely suppress the effect. Here, we are considering lateral, not vertical, coupling of dots. In one sense this reduces the probability of coupling, because of the reduced symmetry of the situation, in the sense that vertically aligned QDs have a large areal overlap that laterally close QDs do not. On the other hand, we are not considering just two dots, but a semi-infinite plane of (laterally organized) dots, which restores the symmetry, and eventually leads to miniband effects. A second difference between vertically and laterally coupled QDs is the tunneling barrier. In vertically coupled QDs, the barrier through which tunneling must occur is the matrix material, whose conduction-band edge lies at energies substantially above those of the dot states. Here, we are not arguing that the dots couple through the matrix, but through the WL, which is made of the same material as the QDs themselves, and has the same conduction-band edge. Thus, we are not considering tunneling of states, which have a lower energy than the conduction-band edge of the "barrier" material, as in vertically coupled dots, but tunneling at energies that are lower energy than those of isolated WL states, but still lie well above the conduction-band edge. A third and crucial difference is that here we are not discussing the coupling of the ground state, but of the excited states, whose lateral extent is typically between 1.5 and 2 times that of the ground state,[20,30] and was recently calculated to be about 66% more extended in isolated InAs/InP QDs grown on a (311)*B* substrate.[31] We can also compare the wave-function penetration in the two cases. For vertically stacked QDs it is into the barrier material, whereas here the wave function spreads out of the dots and into the WL. Indeed, we have shown that for the single-layer high QDD sample the average dot separation is 33 nm, and that the average dot diameter is 26 nm. If we further consider that we are discussing coupling of the more extended excited states, which also are elongated along a particular crystallographic direction (as demonstrated by the polarization), the observation of coupling is very reasonable. A major point made in Ref. 13, that we would also like to emphasize here, is that the problem should be considered, not in terms of islolated QD and quantum-well (WL) systems, but a single quantum-mechanical system, i.e., tending towards a strongly laterally periodically modulated quantum well, in which the lowest energy states nevertheless remain strongly localized and dotlike.

Returning to a more specific description of the various samples reported here, we have seen that for the single-layer samples the lateral ordering is quite weak, which would reduce the miniband effect, and the coupling. On the other hand, as just discussed, the average interdot distance is rather small at 33 nm, and not much larger than the dot diameter, so tunneling via excited states may be expected, even in the absence of strong lateral ordering. For the three and six stacked-layer samples, the inter-QD distance becomes longer [Fig. 2(a)], which decreases the tunneling probability. However, at the same time the degree of lateral ordering and the QD diameter increase, which increases the tunneling probability, compensating for the increase of the inter-QD distance. Indeed, if the QDs are not very near to each other, but strongly laterally ordered, charge carriers can still tunnel, thanks to lattice effects that add a "superperiodicity" to the wave function. Thus the coupling is dependent on the inter-QD distance, the degree of organization, and the QD diameter. These three parameters vary with the number of stacked layers, but in the samples studied here it would seem that the impact of the evolution of one of these parameters is

compensated by the the evolution of another one. Hence, charge-carrier tunneling is always present in all our high QDD samples.

C. Laser thresholds

A complete analysis of laser-threshold currents has been performed in previous works.[22] Threshold-current densities (i.e., current density at which laser emission occurs) are measured to be $J^{T0}_{\text{th high QDD}}=32$ A cm^{-2} for the (C_{T0}) configuration and $J^{T0}_{\text{th low QDD}}=39$ A cm^{-2} for the (U_{T0}) configuration at 110 K (Fig. 8). These threshold currents depend mainly on the gain and the injection efficiency in the active material (QD plane).[1] In a previous work it has been demonstrated, by a quantitative measurement of optical absorption in quantum wells and QDs, that the absorption coefficient, i.e., the material gain, is mainly related to the number of atoms in the active region of InP-based heterostructures.[32] As we mentioned above, the amount of InAs deposited in both high QDD samples and low QDD samples is exactly the same. Measured thresholds at low temperature seem to confirm the absorption measurement as they differ by only 7 A cm^{-2} Thus, assuming that we do not see any thermal effects at this temperature, the material-gain ratio between the high QDD sample and the low QDD sample, corrected for coupling effects on charge redistribution, is then $R_g = g_{\text{high QDD}}/g_{\text{low QDD}}=J^{T0}_{\text{th high QDD}}/J^{T0}_{\text{th low QDD}}=0.82$. In a first approximation, this may lead us to quantify the impact of the coupling on charge redistribution to be about 18%. However, since the number of dots (active centers) can have an influence on gain factor, we refrain from using the difference between threshold currents of the two samples at low temperature to quantify the improvement of charge redistribution efficiency with coupling.

The same measurements have also been performed at room temperature, corresponding to the (U_{RT}) and (C_{RT}) configurations of Fig. 8. Measured threshold-current densities are $J^{\text{RT}}_{\text{th high QDD}}=190$ A cm^{-2} for the (C_{RT}) configuration and $J^{\text{RT}}_{\text{th low QDD}}=520$ A cm^{-2} for the (U_{RT}) configuration.[32] The increase of threshold-current density with temperature is principally due to the thermal excitation of carriers. Electrons that are thermally excited out of the dots will diffuse through the barrier until they are captured by another dot or by an impurity. Assuming the same amount of impurities in both samples, the probability P, to be captured by a dot before meeting an impurity, is then directly linked to the QDD and is increased by a factor of 2 in the high QDD sample, i.e., $P_{\text{capture high QDD}}/P_{\text{capture low QDD}}=2$. Thus, correcting the threshold-current density of the low QDD sample with gain-factor ratio and capture-probability ratio, we find a theoretical expression of the threshold-current density for high QDD sample: $J^{\text{RT}}_{\text{th high QDD}}=R_g (P_{\text{capture low QDD}}/P_{\text{capture high QDD}})$ $J^{\text{RT}}_{\text{th low QDD}}=210$ A cm^{-2}. This is 10% higher than the measured value of 190 A cm^{-2}. This reduction in threshold-current density for the high QDD sample could be interpreted as a direct consequence of the thermally activated tunneling via WL-assisted coupling. Furthermore, we can exclude direct inter-QD coupling (strong-coupling regime), since this is expected to be independent of temperature. Although the estimate is somewhat crude, it does support our assertion that WL-assisted tunneling is beneficial for the performance of QD lasers, which we go on to discuss in more detail in Sec. IV D below. However, it is clear that more research is needed in order to exploit the expected benefits. We stress that the main emphasis of this work is to provide experimental evidence for lateral WL-assisted tunneling, which we have done via the various optical measurements presented above.

D. Advantages of laterally coupled QDs in laser devices

Before concluding we would like to address the implications of using coupled QDs in laser devices. Since lateral coupling is generally considered to produce a degradation of QD properties by removing their zero-dimensional nature, using laterally coupled QDs may not be advantageous for QD laser applications, even though it increases carrier redistribution efficiency: uncoupled dots have a good atomiclike electronic structure, but with lower charge redistribution efficiency. However, the main point demonstrated here is that we can reach an advantageous intermediate coupling regime. This intermediate coupling regime is of prime importance, as it allows us to keep the atomiclike behavior of the grounds tate, which is crucial for the operational advantages of QD lasers, while enhancing the charge-carrier redistribution efficiency due to coupling of excited states. Thus, with this kind of coupling, the electronically optimum situation for lasing (i.e., where every ground state of every QD is occupied) can be reached more easily. Indeed, for a low QDD at low temperature, where many carriers arrive together in a dot, the first two are immediately available to participate in the stimulated emission, while the other carriers occupy excited states. If a neighboring QD is empty, then these carriers cannot redistribute to reach it. In such a configuration, thermodynamic equilibrium seems to be very hard to obtain. In contrast, for the high QDD sample, when many carriers arrive together in a dot, then the first two can participate in the stimulated emission, while the others can rapidly tunnel through the WL to other dots, where they can also contribute to the stimulated emission. Such a sample clearly reaches thermodynamic equilibrium more easily, and so decreases the energy of the whole system. In such a configuration, the internal quantum efficiency of the structure may greatly improve. This improvement of stationary characteristics is not the only benefit of coupled dots in an intermediate coupling regime. It may also lead to significant improvements in carrier dynamics, i.e., intersubband transitions and carrier relaxation.[33] Since coupling between dots implies miniband effects, this should favor relaxation from excited (miniband) states to the 0D ground state. Given that relaxation times are faster in coupled QDs than in uncoupled QDs, coupled-QD lasers may have a better dynamical response to high-frequency modulation (lower chirp, larger frequency bandwidth).

V. CONCLUSIONS

The lateral coupling of QDs and its consequences for charge redistribution in QDs have been studied. It has been

demonstrated that high QD densities can be reached in our InAs/InP system. For such a high QDD, a periodic organization appears and leads to lateral coupling between dots. Evidence of lateral coupling has been determined by measuring a delocalization of the wave function in such dots using magnetophotoluminescence. Miniband effects in excited states arising from the lateral coupling have been shown by polarized photoluminescence. Finally, electroluminescence experiments have been performed on QD laser structures. Improved charge redistribution at low temperature has been demonstrated on high QDD samples, interpreted as a consequence of lateral coupling. This is attributed to inter-QD tunneling of excited states via the wetting layer. It is argued that, as long as the coupling regime is well selected, coupled QDs can improve the efficiency of QD lasers (lower threshold currents), and may also advantageously influence the dynamical characteristics of these devices, by lowering chirp, or increasing the frequency bandwidth.

ACKNOWLEDGMENTS

This work was supported by the EuroMagNET project (Contract No. R113-CT-2004-506239) and the SANDiE Network of Excellence (Contract No. NMP4-CT-2004-500101) of the sixth Framework Programme of the European Commission.

*Email address: charles.cornet@insa-rennes.fr
†Present address: Department of Physics, Lancaster University, Lancaster LA1 4YB, United Kingdom.

[1] D. Bimberg, M. Grundmann, and N. N. Ledentsov, *Quantum Dot Heterostructures* (Chichester, Wiley, 1998).
[2] L. Banyai and S. W. Koch, *Semiconductor Quantum Dots, World Scientific Series on Atomic, Molecular and Optical Physics* (World Scientific, Singapore, New Jersey, London, Hong-Kong, 1993), Vol. 2.
[3] M. Sugawara, *Self-Assembled* InGaAs/GaAs *Quantum Dots, Semiconductors and Semimetals* (Academic, Toronto, 1999), Vol. 60.
[4] Zh. I. Alferov, *Quantum Wires and Dots Show the Way Forward* (Elsevier Science, Oxford, 1998), Vol. 11, p. 47.
[5] S. Varoutsis, S. Laurent, P. Kramper, A. Lemaître, I. Sagnes, I. Robert-Philip, and I. Abram, Phys. Rev. B **72**, 041303(R) (2005).
[6] M. H. Baier, E. Pelucchi, E. Kapon, S. Varoutsis, M. Gallart, I. Robert-Philip, and I. Abram, Appl. Phys. Lett. **84**, 648 (2004).
[7] A. Rastelli, S. Stufler, A. Schliwa, R. Songmuang, C. Manzano, G. Costantini, K. Kern, A. Zrenner, D. Bimberg, and O. G. Schmidt, Phys. Rev. Lett. **92**, 166104 (2004).
[8] J. C. Chen, A. M. Chang, and M. R. Melloch, Phys. Rev. Lett. **92**, 176801 (2004).
[9] H. J. Krenner, M. Sabathil, E. C. Clark, A. Kress, D. Schuh, M. Bichler, G. Abstreiter, and J. J. Finley, Phys. Rev. Lett. **94**, 057402 (2005).
[10] A. Markus, M. Rossetti, V. Calligari, J. X. Chen, and A. Fiore, J. Appl. Phys. **98**, 104506 (2005); M. Sugawara, N. Hatori, H. Ebe, M. Ishida, Y. Arakawa, T. Akyiama, K. Otsubo, and Y. Nakata, *ibid.* **97**, 043523 (2005).
[11] M. Grundmann, Appl. Phys. Lett. **77**, 1428 (2000).
[12] O. Gunawan, H. S. Djie, and B. S. Ooi, Phys. Rev. B **71**, 205319 (2005).
[13] C. Cornet, C. Platz, P. Caroff, J. Even, C. Labbé, H. Folliot, A. Le Corre, and S. Loualiche, Phys. Rev. B **72**, 035342 (2005).
[14] P. Caroff, N. Bertru, A. Le Corre, T. Rohel, I. Alghoraibi, H. Folliot, and S. Loualiche, Jpn. J. Appl. Phys., Part 2 **44**, L1069 (2005).
[15] H. Z. Xu, K. Akahane, H. Z. Song, Y. Okada, and M. Kawabe, J. Cryst. Growth **233**, 639 (2001).
[16] T. V. Lippen, R. Nötzel, G. J. Hamhuis, and J. H. Wolter, Appl. Phys. Lett. **85**, 118 (2004).
[17] J. Tersoff, C. Teichert, and M. G. Lagally, Phys. Rev. Lett. **76**, 1675 (1996).
[18] M. Hayne, J. Maes, S. Bersier, M. Henini, L. Müller-Kirsch, R. Heitz, D. Bimberg, and V. V. Moshchalkov, Physica B **346**, 421 (2004).
[19] S. Raymond, S. Studenikin, A. Sachrajda, Z. Wasilewski, S. J. Cheng, W. Sheng, P. Hawrylak, A. Babinski, M. Potemski, G. Ortner, and M. Bayer, Phys. Rev. Lett. **92**, 187402 (2004).
[20] Y. Sidor, B. Partoens, F. M. Peeters, N. Schildermans, M. Hayne, V. V. Moshchalkov, A. Rastelli, and O. G. Schmidt, Phys. Rev. B **73**, 155334 (2006).
[21] J. Maes, M. Hayne, Y. Sidor, B. Partoens, F. M. Peeters, Y. Gonzalez, L. Gonzalez, D. Fuster, J. M. Garcia, and V. V. Moshchalkov, Phys. Rev. B **70**, 155311 (2004).
[22] A. Patanè, A. Levin, A. Polimeni, L. Eaves, P. C. Main, M. Henini, and G. Hill, Phys. Rev. B **62**, 11084 (2000).
[23] D. G. Deppe and Q. Deng, Appl. Phys. Lett. **73**, 3536 (1998).
[24] P. Caroff, C. Paranthoen, C. Platz, O. Dehaese, H. Folliot, N. Bertru, C. Labbé, R. Piron, E. Homeyer, A. Le Corre, and S. Loualiche, Appl. Phys. Lett. **87**, 243107 (2005).
[25] C. Lobo, R. Leon, S. Marcinkevicius, W. Yang, P. C. Sercel, X. Z. Liao, J. Zou, and D. J. H. Cockayne, Phys. Rev. B **60**, 16647 (1999).
[26] G. S. Solomon, J. A. Trezza, A. F. Marshall, and J. S. Harris, Jr., Phys. Rev. Lett. **76**, 952 (1996); M. Colocci, A. Vinattieri, L. Lippi, F. Bogani, M. Rosa-Clot, S. Taddei, A. Bosacchi, S. Franchi, and P. Frigeri, Appl. Phys. Lett. **74**, 564 (1999); S. Fafard, M. Spanner, J. P. McCaffrey, and Z. R. Wasliewski, *ibid.* **76**, 2268 (2000); J. Maes, M. Hayne, M. Henini, F. Pulizzi, A. Patanè, L. Eaves, and V. V. Moshchalkov, Physica B **346-347**, 428 (2004).
[27] P. Miska, J. Even, C. Paranthoen, O. Dehaese, A. Jbeli, M. Senès, and X. Marie, Appl. Phys. Lett. **86**, 111905 (2005).
[28] M. K. Zundel, P. Specht, K. Eberl, N. Y. Jin-Phillipp, and E. Phillipp, Appl. Phys. Lett. **71**, 2972 (1997); R. Provoost, M. Hayne, V. V. Moshchalkov, M. K. Zundel, and K. Eberl, *ibid.* **75**, 799 (1999).
[29] Y. D. Jang, E. G. Lee, J. S. Yim, D. Lee, W. G. Jeong, S. H. Pyun, and J. W. Wang, Appl. Phys. Lett. **88**, 091920 (2006).
[30] O. Stier, M. Grundmann, and D. Bimberg, Phys. Rev. B **59**, 5688

(1999); F. Guffarth, R. Heitz, A. Schliwa, O. Stier, N. N. Ledentsov, A. R. Kovsh, V. M. Ustinov, and D. Bimberg, *ibid.* **64**, 085305 (2001).

[31] C. Cornet, A. Schliwa, J. Even, F. Doré, C. Celebi, A. Létoublon, E. Macé, C. Paranthoën, A. Simon, P. M. Koenraad, N. Bertru, D. Bimberg, and S. Loualiche, Phys. Rev. B **74**, 035312 (2006).

[32] C. Cornet, C. Labbé, H. Folliot, N. Bertru, O. Dehaese, J. Even, A. Le Corre, C. Paranthoen, C. Platz, and S. Loualiche, Appl. Phys. Lett. **85**, 5685 (2004).

[33] C. Cornet, C. Labbé, H. Folliot, P. Caroff, C. Levallois, O. Dehaese, J. Even, A. Le Corre, and S. Loualiche, Appl. Phys. Lett. **88**, 171502 (2006).